

GEOMETRICALLY LINEAR/NONLINEAR SANDWICH STRUCTURES WITH ANISOTROPIC FACE SHEETS: THEORY AND BEHAVIOR

Liviu Librescu and Terry Hause
Virginia Polytechnic Institute and State University
Department of Engineering Science and Mechanics
Blacksburg, Virginia 24061, USA

Keywords: *Anisotropic Sandwich Shells, Weak Core, Postbuckling, Load Carrying Capacity, Buckling Strength*

Abstract

This paper is focussed on the formulation of a comprehensive geometrically nonlinear theory of shallow sandwich shells that includes also the effect of the initial geometric imperfections. It is assumed that the face-sheets of the sandwich structure are built-up from anisotropic material layers. Both strong and weak core sandwich structures are considered. As a result of its features, the developed structural model can provide important information related to the load carrying capacity of sandwich structures in the pre- and postbuckling ranges. Moreover, by using the directionality properties of face-sheet materials, ways to enhance the load carrying capacity of sandwich shells/plates, without weight penalties, and in both the linear and nonlinear regimes are reached. Selected numerical illustrations emphasizing the implications of these non-classical features are presented and pertinent conclusions are outlined.

1 Introduction

A typical laminated composite structure that due to its outstanding properties is likely to play a great role in the construction of advanced supersonic/hypersonic space vehicles and of future reusable space transportation systems is the sandwich-type construction.

The sandwich structures exhibit a number of features of exceptional importance such as: i) increased bending-stiffness with little resultant weight penalty, ii) excellent thermal and sound insulation as well as a smooth aerodynamic surface in a higher-speed flow environment, and iii) extended operational life as compared to stiffened-reinforced structures that are weakened by the appearance of stress concentration.

It clearly appears that due to these features, the sandwich structures can play also an important role in the design of advanced marine structures, and in the construction of communication satellite antennas and reflectors, as well.

One of the problems which, for a better understanding and exploitation of their load carrying capacity is essential, is that associated with the determination of the postbuckling behavior of curved sandwich panels under complex loading conditions.

In addition to general conclusions related to the capacity of these structures to carry thermomechanical loadings, this study will supply, among others, pertinent information about the sensitivity of the load carrying capacity of these structures to initial geometric imperfection, about the conditions of the occurrence of the snap-through buckling, of its severity, and conditions in which it can be attenuated or even suppressed

altogether, as well on a number of other issues that are essential for a reliable design and exploitation of these structures.

Under the present study, the sandwich structure consists of a thick core-layer bonded by the face-sheets that consist of composite anisotropic materials, symmetrically laminated with respect to the mid-surface of the core-layer. The initial geometric imperfection consisting of a stress free initial transversal deflection, will be also incorporated in the study. The loads under which the postbuckling response will be analyzed consist of uniaxial/biaxial compressive edge loads and a non-uniform thermal field.

In spite of the evident importance of the problems considered in this study, relatively few results on these issues have been considered in the specialized literature. The available survey papers (see e.g. Refs. 1 and 2) on this topic can provide pertinent references to these problems.

It should also be mentioned that the theory presented in this paper has been developed in a series of previous work (see Refs. 2 through 8).

2 Basic Assumptions and Conventions

The global middle surface of the structure σ , selected to coincide with that of the core layer, is referred to a curvilinear and orthogonal coordinate system x_α ($\alpha = 1, 2$). The normal thicknesswise coordinate x_3 is considered positive when measured in the direction of the inward normal. The uniform thickness of the core is $2\bar{h}$ while those of the bottom and top faces are h'' and h' , respectively. As a result, H ($\equiv 2\bar{h} + h' + h''$) is the total thickness of the structure (see Fig. 1).

For the sake of identification, the quantities affiliated with the core layer will be marked by a superposed bar, while those associated with lower and upper faces by a single and double primes, respectively, placed on the right or left of the respective quantity. The geometrically non-linear theory of doubly curved sandwich shells developed in the framework of the Lagrangian description is based on a number of assumptions, such as: i) the face-sheets are built-up from orthotropic material layers, the axes of orthotropy

of the individual plies being not necessarily coincident with the geometrical axes x_α of the structure, ii) the material of the core layer features orthotropic properties, the axes of orthotropy being parallel to the geometrical axes x_α .

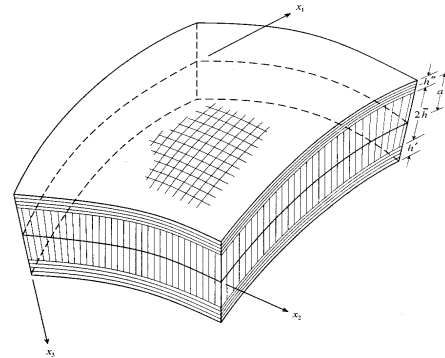


Fig. 1 Doubly-curved sandwich panel

The thickness of the core layer is assumed to be much larger than those of the face sheets, i.e. $2\bar{h} \gg h', h''$. The theory encompasses the cases of *weak* and *strong* core sandwich structures, as well. In this respect it should be recalled that in the former case the core is capable of carrying transverse shear stresses only, whereas in the latter one, the core can carry both tangential and transverse shear stresses, iii) a perfect bonding between the face sheets and between the faces and the core is postulated, iv) the incompressibility in the transverse normal direction is postulated in both the core and face-sheets, v) the principle of shallow shell theory is adopted.

3 Kinematics

Upon adopting a linear distribution of the tangential displacement components across the thickness of the face-sheets and core, and fulfilling the kinematic continuity conditions at the interface between the core and face-sheets, in conjunction with assumption iv), the 3-D displacement components result in the following representations:

$$\left. \begin{aligned} V_1(x_\alpha, x_3) &= \xi_1(x_\alpha) + \eta_1(x_\alpha) + (x_3 - a') \psi_1(x_\alpha) \\ V_2(x_\alpha, x_3) &= \xi_2(x_\alpha) + \eta_2(x_\alpha) + (x_3 - a') \psi_2(x_\alpha) \\ V_3(x_\alpha, x_3) &= v_3(x_\alpha) \end{aligned} \right\} \quad \text{valid for } \bar{h} \leq x_3 \leq \bar{h} + h' \quad (1a-c)$$

4 Equations of Equilibrium/Motion and Boundary Conditions

$$\left. \begin{aligned} \bar{V}_1(x_\alpha, x_3) &= \xi_1(x_\alpha) - \frac{1}{4}[h'\psi_1'(x_\alpha) - h''\psi_1''(x_\alpha)] \\ &\quad + (x_3/\bar{h})\{\eta_1(x_\alpha) - \frac{1}{4}[h'\psi_1'(x_\alpha) + h''\psi_1''(x_\alpha)]\} \\ \bar{V}_2(x_\alpha, x_3) &= \xi_2(x_\alpha) - \frac{1}{4}[h'\psi_2'(x_\alpha) + h''\psi_2''(x_\alpha)] \\ &\quad + (x_3/\bar{h})\{\eta_2(x_2) - \frac{1}{4}[h'\psi_2'(x_\alpha) + h''\psi_2''(x_\alpha)]\} \\ \bar{V}_3(x_\alpha, x_3) &= v_3(x_\alpha) \end{aligned} \right\} \text{valid for and } -\bar{h} \leq x_3 \leq \bar{h} \quad (2a-c)$$

$$\left. \begin{aligned} {}''V_1(x_\alpha, x_3) &= \xi_1(x_\alpha) - \eta_1(x_\alpha) + (x_3 + a'')''\psi_1(x_\alpha) \\ {}''V_2(x_\alpha, x_3) &= \xi_2(x_\alpha) - \eta_2(x_\alpha) + (x_3 + a'')''\psi_2(x_\alpha) \\ {}''V_3(x_\alpha, x_3) &= v_3(x_\alpha) \end{aligned} \right\} \text{valid for } -\bar{h} - h'' \leq x_3 \leq \bar{h} \quad (3a-c)$$

In these equations the 2-D tangential displacement measures $\xi_\alpha(x_1, x_2)$ and $\eta_\alpha(x_1, x_2)$ are defined as:

$$\begin{aligned} \xi_1 &= ({}'V_1^\circ + {}''V_1^\circ)/2, \eta_1 = ({}'V_1^\circ - {}''V_1^\circ)/2, \\ \xi_2 &= ({}'V_2^\circ + {}''V_2^\circ)/2, \eta_2 = ({}'V_2^\circ - {}''V_2^\circ)/2. \end{aligned} \quad (4a-d)$$

where $'V_\alpha^\circ$, ψ_α' ; $''V_\alpha^\circ$, ψ_α'' and \bar{V}_α° , $\bar{\psi}_\alpha$ denote the tangential displacements of the points of the mid-surface and the shear angle rotations of the bottom, upper face-sheets and of the core layer, respectively, while $a'(\equiv \bar{h} + h'/2)$ and $a''(\equiv \bar{h} + h''/2)$ denote the distances between the global mid-surface (coinciding with core mid-surface) and the mid-surfaces of the bottom and top faces, respectively. As a result, the 2-D displacement measures reduce to nine functions, namely ξ_1 , ξ_2 , η_1 , η_2 , v_3 , $'\psi_1$, $'\psi_2$, $''\psi_1$ and $''\psi_2$. Assuming that the structure features also a stress-free initial geometric imperfection $\bar{V}_3^\circ(\equiv \bar{v}_3^\circ(x_\alpha))$, and adopting the concept of small strains and moderately small rotations (see Ref. 11), the following strain distribution is across the top and bottom face sheets and of the core layer. These equations are not displayed here.

The equations of equilibrium/motion and the boundary conditions are obtained via application of Hamilton's variational principle. As a result of its application, upon retaining only the transversal load and transverse inertia terms, the equations of motion expressed in terms of global stress resultants and stress couples are:

$$\begin{aligned} \delta\xi_1 : N_{11,1} + N_{12,2} &= 0, \\ \delta\xi_2 : N_{22,2} + N_{12,1} &= 0, \\ \delta\eta_1 : L_{11,1} + L_{12,2} - \bar{N}_{13} &= 0, \\ \delta\eta_2 : L_{22,2} + L_{12,1} - \bar{N}_{23} &= 0, \\ \delta\psi_1' : \hat{H}_{11,1} + \hat{H}_{12,2} + N'_{13} - (h'/4\bar{h})\bar{N}_{13} &= 0, \\ \delta\psi_2' : \hat{H}_{22,2} + \hat{H}_{12,1} + N'_{23} - (h'/4\bar{h})\bar{N}_{23} &= 0, \end{aligned} \quad (5)$$

$$\begin{aligned} \delta\psi_1'' : \hat{H}_{11,1} + \hat{H}_{12,2} + N''_{13} + (h''/4\bar{h})\bar{N}_{13} &= 0, \\ \delta\psi_2'' : \hat{H}_{22,2} + \hat{H}_{12,1} + N''_{23} - (h''/4\bar{h})\bar{N}_{23} &= 0, \\ \delta v_3 : N_{11} \left(v_{3,11} + \overset{\circ}{v}_{3,11} + 1/R_1 \right) + 2N_{12} \left(v_{3,12} \right. \\ &\quad \left. + \overset{\circ}{v}_{3,12} \right) + N_{22} \left(v_{3,22} + \overset{\circ}{v}_{3,22} + 1/R_2 \right) \\ &\quad + N_{13,1} + N_{23,2} + q_3 - m_o \ddot{v}_3 = 0. \end{aligned}$$

For more details related with the derivation of these equations, see Refs. 7 and 8. Herein $1/R_1$ and $1/R_2$ denote the principal curvatures of the global middle surface, $(\cdot)_{,\alpha} (\equiv \partial(\cdot)/\partial x_\alpha)$ denotes the partial differentiation with respect to the surface coordinate x_α , q_3 is the distributed transversal load, while m_o denotes the reduced mass per unit area of the shell mid-surface. As concerns the global stress resultants and stress couples in terms of which Eqs. (8) are expressed, these are defined as:

$$\begin{aligned} N_{11} &= N'_{11} + \bar{N}_{11} + N''_{11}, \quad (1 \leftrightarrow 2) \\ N_{12} &= N'_{12} + \bar{N}_{12} + N''_{12}, \\ N_{13} &= N'_{13} + \bar{N}_{13} + N''_{13}, \quad (1 \leftrightarrow 2) \\ L_{11} &= \bar{h}(N'_{11} - N''_{11}) + \bar{M}_{11}, \quad (1 \leftrightarrow 2) \\ L_{12} &= \bar{h}(N'_{12} - N''_{12}) + \bar{M}_{12} \end{aligned} \quad (6)$$

$$\begin{aligned}\hat{H}_{11} &= (h'/4) (\bar{N}_{11} + \bar{M}_{11}/\bar{h}) - M'_{11}, \left(1 \overleftrightarrow{2}\right) \\ \hat{H}_{12} &= (h'/4) (\bar{N}_{12} + \bar{M}_{12}/\bar{h}) - M'_{12}, \\ \hat{H}_{11} &= (h''/4) (\bar{N}_{11} - \bar{M}_{11}/\bar{h}) + M''_{11}, \left(1 \overleftrightarrow{2}\right) \\ \hat{H}_{12} &= (h''/4) (\bar{N}_{12} - \bar{M}_{12}/\bar{h}) + M''_{12},\end{aligned}$$

Herein the sign $\left(1 \overleftrightarrow{2}\right)$ indicates that the expressions of the stress resultants and stress couples not explicitly written can be obtained from the ones displayed above, upon replacing subscript 1 by 2 and vice-versa.

Consistent with the concept of shallow shell theory, the stress resultants and stress couples associated with the top face-sheets and the core that intervene in Eqs. (5) and (6) are:

$$\begin{aligned}\{N'_{\alpha\beta}, M'_{\alpha\beta}\} \\ = \sum_{k=1}^{n'} \int_{(x_3)_{k-1}}^{(x_3)_k} '(S_{\alpha\beta})_k \{1, x_3 - 'a\} dx_3,\end{aligned}\quad (7)$$

$$\begin{aligned}N'_{\alpha 3} &= \sum_{k=1}^{n'} \int_{(x_3)_{k-1}}^{(x_3)_k} '(S_{\alpha 3})_k dx_3, \\ (\alpha, \beta &= 1, 2)\end{aligned}$$

and

$$\{\bar{N}_{\alpha\beta}, \bar{M}_{\alpha\beta}\} = \int_{-\bar{h}}^{\bar{h}} \bar{S}_{\alpha\beta} \{1, x_3\} dx_3,\quad (8)$$

$$\bar{N}_{\alpha 3} = \int_{-\bar{h}}^{\bar{h}} \bar{S}_{\alpha 3} dx_3,$$

respectively.

The stress resultants and stress couples associated with the top facings can be obtained from Eqs. (7) by replacing single primes by double primes, a' by $-a''$ and n' by n'' . Herein, n' and n'' denote the number of layers constituent to the bottom and top facings, respectively, while $(x_3)_k$ and $(x_3)_{k-1}$ denote the distances from the global reference surface (coinciding with that of the core layer) to the upper and bottom interfaces of the k th layer, respectively. These definitions of

stress resultants and stress couples are similar to the ones in Refs. [5] and [6].

The associated boundary conditions at the edge $x_n = \text{constant}$, ($n = 1, 2$), obtained also from Hamilton's variational principle are:

$$\begin{aligned}N_{nn} &= \underline{N}_{nn} \text{ or } \xi_n = \underline{\xi}_n \\ N_{nt} &= \underline{N}_{nt} \text{ or } \xi_t = \underline{\xi}_t \\ L_{nn} &= \underline{L}_{nn} \text{ or } \eta_n = \underline{\eta}_n \\ L_{nt} &= \underline{L}_{nt} \text{ or } \eta_t = \underline{\eta}_t \\ \hat{H}_{nn} &= \hat{\underline{H}}_{nn} \text{ or } \psi'_n = \underline{\psi}'_n \\ \hat{H}_{nt} &= \hat{\underline{H}}_{nt} \text{ or } \psi'_t = \underline{\psi}'_t \\ \hat{H}_{nn} &= \hat{\underline{H}}_{nn} \text{ or } \psi''_n = \underline{\psi}''_n \\ \hat{H}_{nt} &= \hat{\underline{H}}_{nt} \text{ or } \psi''_t = \underline{\psi}''_t \\ N_{nt}(v_{3,t} + \overset{\circ}{v}_{3,t}) + N_{nn}(v_{3,n} \text{ or } v_3 = v_3 \\ &\quad + \overset{\circ}{v}_{3,n}) + N_{n3} = \underline{N}_{n3}\end{aligned}\quad (9)$$

Herein the subscripts n and t are used to designate the normal and tangential in-plane directions to an edge and hence, $n = 1$ when $t = 2$, and vice-versa, $n = 2$ when $t = 1$. In addition, the quantities underscored by a tilde denote prescribed quantities. It should be remarked that the above equations incorporate transverse shear deformability of face sheets and the strong core features.

In the case of the soft core sandwich structures, $\bar{N}_{\alpha\beta}$ and $\bar{M}_{\alpha\beta}$ should be considered zero-valued quantities in the expressions of the global stress resultants and stress couples, Eqs. (9) and (10).

5 Constitutive Equations

Toward the goal of deriving the 2-D constitutive equations within the theory of sandwich shells, it should be recalled that within the 3-D geometrically non-linear elasticity theory, the constitutive equations are described by linear relationships between the second Piola-Kirchhoff stress

and Lagrange strain tensor components (see Ref. 9).

As a result, for an anisotropic material featuring monoclinic symmetry and including the temperature and moisture effects, the generalized Hooke's law can be expressed as:

$$\begin{aligned} \begin{Bmatrix} S_{11} \\ S_{22} \\ S_{12} \end{Bmatrix} &= \begin{bmatrix} \hat{Q}_{11} & \hat{Q}_{12} & \hat{Q}_{16} \\ \hat{Q}_{12} & \hat{Q}_{22} & \hat{Q}_{26} \\ \hat{Q}_{16} & \hat{Q}_{26} & \hat{Q}_{66} \end{bmatrix} \begin{Bmatrix} e_{11} \\ e_{22} \\ 2e_{12} \end{Bmatrix} \\ &- \begin{Bmatrix} \hat{\lambda}_1 \\ \hat{\lambda}_2 \\ \hat{\lambda}_6 \end{Bmatrix} T - \begin{Bmatrix} \hat{\mu}_1 \\ \hat{\mu}_2 \\ \hat{\mu}_6 \end{Bmatrix} M, \begin{Bmatrix} S_{23} \\ S_{13} \end{Bmatrix} \\ &= K^2 \begin{bmatrix} Q_{44} & Q_{45} \\ Q_{45} & Q_{55} \end{bmatrix} \begin{Bmatrix} 2e_{23} \\ 2e_{13} \end{Bmatrix} \end{aligned} \quad (10)$$

In these equations S_{ij} denotes second Piola-Kirchhoff stress tensor, \hat{Q}_{ij} ($\equiv Q_{ij} - \frac{Q_{i3}Q_{j3}}{Q_{33}}$) are the reduced elastic moduli, $\hat{\lambda}_I$ ($\equiv \lambda_I - \frac{Q_{I3}}{Q_{33}}\lambda_{33}$) and $\hat{\mu}_I$ ($\equiv \mu_I - \frac{Q_{I3}}{Q_{33}}\mu_{33}$) denote the reduced thermal expansion and moisture swelling coefficients, respectively, where T ($\equiv T(x_\alpha, x_3)$) and M ($\equiv M(x_\alpha, x_3)$) denote the excess of temperature and moisture with respect to the free stress temperature and moisture T_r and M_r , respectively. Herein the index I takes the values 1, 2 or 6.

Since the anisotropic material featuring a monoclinic symmetry can simulate an orthotropic material whose axes of orthotropy are rotated with respect to the geometrical axes of the structure, the elastic, thermal and moisture moduli, \hat{Q}_{ij} , $\hat{\lambda}_I$ and $\hat{\mu}_I$, respectively, can be expressed in terms of the associated elastic, thermal expansion and moisture swelling moduli in the on-axis configuration and the angles by which the principle material axes are rotated with respect the geometrical ones (i.e. the ply angles).

Employment in Eqs. (10) of (7), results in the constitutive equations for the bottom face-sheets.

Expressed in compact form these are:

$$\begin{aligned} {}'N_{11} &= A'_{11}\epsilon'_{11} + A'_{12}\epsilon'_{22} + A'_{16}\gamma'_{12} + E'_{11}\kappa'_{11} \\ &\quad + E'_{12}\kappa'_{22} + E'_{16}\kappa'_{12} - {}'N_{11}^T - {}'N_{11}^m, \quad (1 \leftrightarrow 2) \\ {}'N_{12} &= A'_{16}\epsilon'_{11} + A'_{26}\epsilon'_{22} + A'_{66}\gamma'_{12} + E'_{16}\kappa'_{11} \\ &\quad + E'_{26}\kappa'_{22} + E'_{66}\kappa'_{12} - {}'N_{12}^T - {}'N_{12}^m, \\ {}'N_{23} &= {}'K^2 [{}'A_{44}\gamma'_{23} + {}'A_{45}\gamma'_{13}], \quad (11) \\ {}'N_{13} &= {}'K^2 [{}'A_{45}\gamma'_{23} + {}'A_{55}\gamma'_{13}], \\ {}'M_{11} &= E'_{11}\epsilon'_{11} + E'_{12}\epsilon'_{22} + E'_{16}\gamma'_{12} + F'_{11}\kappa'_{11} \\ &\quad + F'_{12}\kappa'_{22} + F'_{16}\kappa'_{12} - {}'M_{11}^T - {}'M_{11}^m, \quad (1 \leftrightarrow 2) \\ {}'M_{12} &= E'_{16}\epsilon'_{11} + E'_{26}\epsilon'_{22} + E'_{66}\gamma'_{12} + F'_{16}\kappa'_{11} \\ &\quad + F'_{26}\kappa'_{22} + F'_{66}\kappa'_{12} - {}'M_{12}^T - {}'M_{12}^m. \end{aligned}$$

The stiffness quantities appearing in Eqs. (11) are defined as

$$\begin{aligned} &\{A'_{\omega\rho}, B'_{\omega\rho}, D'_{\omega\rho}\} \\ &= \sum_{k=1}^{n'} \int_{(x_3)_{k-1}}^{(x_3)_k} (\hat{Q}'_{\omega\rho})_{(k)} (1, x_3, x_3^2) dx_3, \\ &\quad (\omega, \rho = 1, 2, 6) \\ A'_{IJ} &= {}'K^2 \sum_{k=1}^{n'} \int_{(x_3)_{k-1}}^{(x_3)_k} (Q'_{IJ}) dx_3, \quad (I, J = 4, 5) \\ {}'N_{\alpha\beta}^T &= \sum_{k=1}^{n'} \int_{(x_3)_{k-1}}^{(x_3)_k} (\hat{\lambda}'_{\alpha\beta})_k T dx_3, \\ {}'N_{\alpha\beta}^m &= \sum_{k=1}^{n'} \int_{(x_3)_{k-1}}^{(x_3)_k} (\hat{\mu}'_{\alpha\beta})_k M dx_3 \quad (12) \\ {}'M_{\alpha\beta}^T &= \sum_{k=1}^{n'} \int_{(x_3)_{k-1}}^{(x_3)_k} (x_3 - a') (\hat{\lambda}'_{\alpha\beta})_k T dx_3, \\ {}'M_{\alpha\beta}^m &= \sum_{k=1}^{n'} \int_{(x_3)_{k-1}}^{(x_3)_k} (x_3 - a') (\hat{\mu}'_{\alpha\beta})_k M dx_3, \\ &\quad (\alpha, \beta = 1, 2) \end{aligned}$$

while

$$\begin{aligned} E'_{\omega\rho} &= B'_{\omega\rho} - a'A'_{\omega\rho}, \\ F'_{\omega\rho} &= D'_{\omega\rho} - 2a'B'_{\omega\rho} + a'^2 A'_{\omega\rho} \quad (13a,b) \end{aligned}$$

The expression of stress resultants and stress couples for the top facings can be obtained from Eqs. (11) and (12) by replacing the single prime

by double primes. In the case when bottom and upper facings feature full symmetry about their own mid-surfaces, $E'_{\omega p} \equiv 0$ and $E''_{\omega p} \equiv 0$.

For the core layer considered as an orthotropic body (the axes of orthotropy coinciding with the geometrical axes), the constitutive equations are:

$$\begin{aligned}\bar{N}_{11} &= 2\bar{h} [\bar{Q}_{11}\bar{\epsilon}_{11} + \bar{Q}_{12}\bar{\epsilon}_{22}] \\ &\quad - \bar{N}_{11}^T - \bar{N}_{11}^m, \quad (1 \leftrightarrow 2) \\ \bar{N}_{12} &= 2\bar{h} \bar{Q}_{66}\bar{\gamma}_{12}, \\ \bar{N}_{13} &= 2\bar{h} \bar{K}^2 \bar{Q}_{55}\bar{\gamma}_{13}, \quad (1 \leftrightarrow 2) \quad (14a-e) \\ \bar{M}_{11} &= \frac{2}{3}\bar{h}^3 [\bar{Q}_{11}\bar{\kappa}_{11} + \bar{Q}_{12}\bar{\kappa}_{22}] \\ &\quad - \bar{M}_{11}^T - \bar{M}_{11}^m, \quad (1 \leftrightarrow 2) \\ \bar{M}_{12} &= \frac{2}{3}\bar{h}^3 \bar{Q}_{66}\bar{\kappa}_{12},\end{aligned}$$

where

$$\begin{aligned}\left(\bar{N}_{\alpha\beta}^T, \bar{M}_{\alpha\beta}^T\right) &= \int_{-\bar{h}}^{\bar{h}} (1, x_3) \bar{\lambda}_{\alpha\beta} T dx_3, \\ &\quad (\alpha, \beta = 1, 2) \\ \left(\bar{N}_{\alpha\beta}^m, \bar{M}_{\alpha\beta}^m\right) &= \int_{-\bar{h}}^{\bar{h}} (1, x_3) \bar{\mu}_{\alpha\beta} M dx_3. \quad (15a,b)\end{aligned}$$

In Eqs. (11), (12) and (14), $'K^2$ and \bar{K}^2 denote transverse shear correction factors associated with the facings and core, respectively. Notice that Eqs. (14) correspond to a strong core sandwich structure. In the case of a soft core sandwich structure, with the exception of \bar{N}_{13} and \bar{N}_{23} , all the remaining stress resultants and stress couples associated with the core layer become immaterial.

6 Governing Equations

One possible and most straightforward representation of the governing equations in the theory of shells, in general, and of sandwich-type structures, in particular, is that in terms of displacement quantities. However, as the recent results in

the area reveal, the mixed formulation of shear deformable shallow shell theory (i.e. that in terms of the Airy's potential function, transversal deflection and of a transverse shear potential function), presents many advantages, especially toward the study of their buckling and postbuckling response (see e.g. Refs. 12 and 13). For sandwich structures, however, this type of formulation works well only in special cases.

As in the general case of shells, the governing equations of sandwich structures can be represented in terms of displacement, or mixed quantities. Whereas the formulation in terms of displacement quantities was established in a rather general framework and used in Ref. 10, that in terms of mixed quantities, (i.e., in terms of an Airy's potential function, transversal deflection and a transverse shear potential function), was established in the framework of a simplified sandwich shell theory. The simplifications involve: a) adoption of the weak core model, b) thin face-sheets that enables one to discard transverse shear effects, and c) local and global symmetrically laminated face-sheets. In this case the stress resultants $N_{\alpha\beta}$ can be expressed as

$$N_{\alpha\beta} = c_{\alpha\rho} c_{\beta\sigma} \phi_{,\rho\sigma} \quad (16)$$

where $c_{\alpha\beta}$ stands for the 2-D antisymmetric tensor while ϕ is the Airy's function. Enforcing the conditions of symmetry that yield

$$A'_{\alpha\beta} = A''_{\alpha\rho} \equiv A_{\alpha\beta}, \quad F'_{\alpha\beta} = F''_{\alpha\rho} \equiv F_{\alpha\beta},$$

$$E'_{\alpha\beta} = E''_{\alpha\beta} = 0, \quad a' = a'' \equiv a; \quad h' = h'' \equiv h,$$

the governing equations result as

$$\begin{aligned}A_{11}\eta_{1,11} + A_{16}\eta_{2,11} + A_{66}\eta_{1,22} + (A_{12} + A_{66})\eta_{2,12} \\ + 2A_{16}\eta_{1,12} + A_{26}\eta_{2,22} \\ - (2\bar{K}^2\bar{G}_{13}/\bar{h})(\eta_1 + av_{3,1}) = 0, \quad (1 \leftrightarrow 2) \\ \phi_{,22}(v_{3,11} + \overset{\circ}{v}_{3,11} + 1/R_1) + \phi_{,11}(v_{3,22} + \overset{\circ}{v}_{3,22} \\ + 1/R_2) - 2\phi_{,12}v_{3,12} + \overset{\circ}{v}_{3,12} \\ - F_{11}v_{3,1111} - F_{22}v_{3,2222} - 4F_{16}v_{3,1112} \\ - 4F_{26}v_{3,1222} - 2(F_{12} + 2F_{66})v_{3,1122} \\ + (2\bar{K}^2a/\bar{h})\{\bar{G}_{13}(\eta_{1,1} \\ + av_{3,11}) + \bar{G}_{23}(\eta_{2,2} + av_{3,22})\} + q_3 \\ - m_0\overset{\circ}{v}_3 = 0. \quad (17a,b)\end{aligned}$$

Recalling that the equations of equilibrium (5a,b) are identically fulfilled via the use of the stress potential function ϕ given by Eq. (16), in order to ensure single valued displacements, the compatibility equation for the membrane strains has to be satisfied as well.

For the problem at hand the compatibility equation is:

$$\begin{aligned} \varepsilon_{11,22} + \varepsilon_{22,11} - \gamma_{12,12} + (2/R_1)v_{3,22} + (2/R_2)v_{3,11} \\ - 2v_{3,12}^2 + 2v_{3,11}v_{3,22} + 2\overset{\circ}{v}_{3,11}v_{3,22} \\ - 4v_{3,12}\overset{\circ}{v}_{3,12} + 2v_{3,11}\overset{\circ}{v}_{3,22} = 0, \end{aligned} \quad (18)$$

where

$$\begin{aligned} \varepsilon_{11} &= {}' \varepsilon_{11} + {}'' \varepsilon_{11}, \quad \varepsilon_{22} = {}' \varepsilon_{22} + {}'' \varepsilon_{22}, \\ \gamma_{12} &= {}' \gamma_{12} + {}'' \gamma_{12}. \end{aligned}$$

In order to express this equation in terms of the basic unknown functions, a partial inversion of constitutive equations (14a), has to be carried out. With the use of these equations, Eq. (18) reduces to

$$\begin{aligned} A_{22}^* \phi_{,1111} + A_{11}^* \phi_{,2222} - 2A_{16}^* \phi_{,1222} - 2A_{26}^* \phi_{,2111} \\ + (A_{66}^* + 2A_{12}^*) \phi_{,1122} + (2/R_1)v_{3,22} \\ + (2/R_2)v_{3,11} - 2v_{3,12}^2 + 2v_{3,11}v_{3,22} \quad (19) \\ + 2\overset{\circ}{v}_{3,11}v_{3,22} + 2v_{3,11}\overset{\circ}{v}_{3,22} - 4v_{3,12}\overset{\circ}{v}_{3,12} = 0. \end{aligned}$$

As a result, the equations for the problem at hand reduces to four partial differential equations expressed in terms of the functions η_1 , η_2 , v_3 and ϕ .

In Eq. (19), the stiffness quantities

$${}' A_{\omega\rho}^* = {}'' A_{\omega\rho}^* \equiv A_{\omega\rho}^* \quad (\omega, \rho = 1, 2, 6) \quad (20)$$

where ${}' A_{\omega\rho}^*$ and ${}'' A_{\omega\rho}^*$ represent the inverted counterparts of ${}' A_{\omega\rho}$ and ${}'' A_{\omega\rho}$, respectively. In these equations, for the sake of simplifications, the temperature and moisture effects have been discarded.

7 Numerical Simulations

The selected numerical results that will be supplied, have the goal of highlighting the influence

of a number of effects on the buckling strength and the nonlinear response. The materials used to generate the results that concern flat and curved sandwich panels can be found in Ref. 9..

7.1 Effects of the ply-angle in the face-sheets and of panel aspect ratio on the buckling strength.

In Figs. 2 and 3 there are depictions of the variation of the buckling load in uniaxial compression vs. ply-angle of the face-sheet material, for a sandwich flat panel of various aspect ratios $\Psi (\equiv L_2/L_1)$

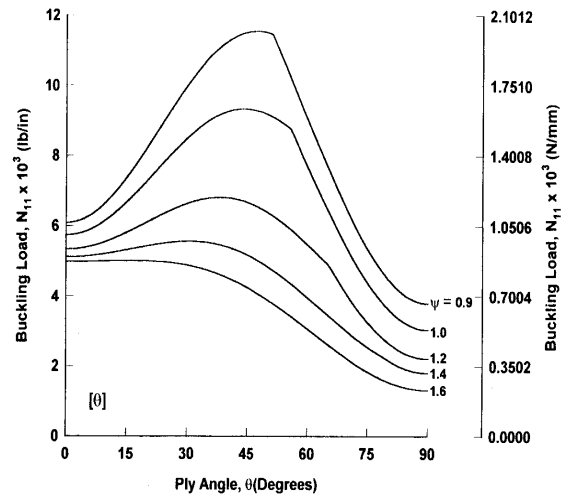


Fig. 2 The influence of the fiber orientation in the face-sheets on the uniaxial compressive buckling strength of a sandwich flat panel. Each of the faces consists of one ply. All four edges are movable. $L_1 = 24$ in., $h_f = 0.02$ in., $h_c = 0.5$ in., Materials F1:C1

In both cases the panel consists of an Aluminum Honeycomb core (labeled C1) and facings made up from HS Graphite Epoxy (labeled F1). (See Ref. 9 for the elastic properties of materials used). The selected material of face-sheets, is characterized by a rather large orthotropy ratio. Each face sheets of the sandwich panel considered in Fig. 2 is made up from one layer, in contrast to the panel in Fig. 3, for which each face-sheet consists of three plies. It is also assumed that in both cases the thickness of face-sheets remains unchanged. From these

two plots, it becomes evident that for any considered panel aspect ratio, an increase of the number of layers in each face-sheet, without the increase of their thickness, is accompanied by a slight increase of the buckling strength.

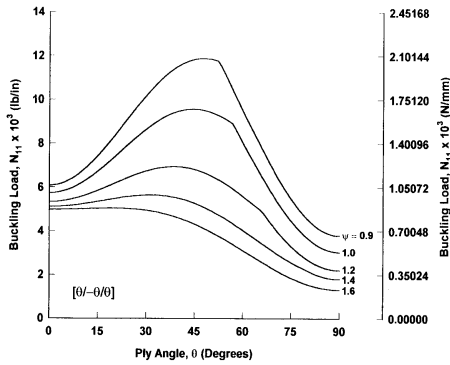


Fig. 3 The counterpart of Fig. 2. In this case, each face-sheets is made up from three layers in the sequence $[\theta/-\theta/\theta]$. The total thickness of each of the faces is the same as in Fig. 2. ($L_1 = 23$ in., $h_f = 0.02$ in., $h_c = 0.5$ in., Materials F1:C1).

The results shown in Figs. 2 and 3 also reveal that for aspect ratios $\psi \leq 1$, the buckling strength is more sensitive to the variation of ply-angle than for the panels of aspect ratio $\psi > 1$. In addition, from Figs. 2 and 3 it becomes apparent that with the increase of the panel aspect ratio, both a decay of the maximum buckling strength and a shift of the corresponding ply-angle towards smaller angles are experienced.

Notice that in these two plots, for any $\psi \leq 1.2$, the minimum buckling load prior to the first discontinuities have been determined for $m = n = 1$, whereas the remaining parts of the curves have been determined for $m = 2, n = 1$. However, for $\psi > 1.2$, there are not changes in the mode number for the minimum buckling load, i.e. in this case this condition is obtained throughout for $m = n = 1$.

In Figs. 4 and 5, the buckling strength of a three-ply flat and of a circular cylindrical panel counterpart is displayed. As it can be seen, for the same ply-angle the cylindrical sandwich panel is able to carry larger compressive edge loads than its flat panel counterpart.

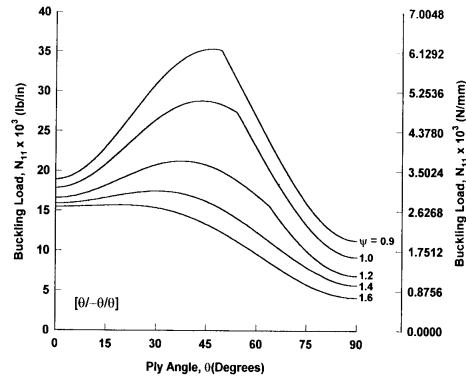


Fig. 4 The counterpart of Fig. 3, where each of the face-sheets is three times thicker than in Fig. 3.

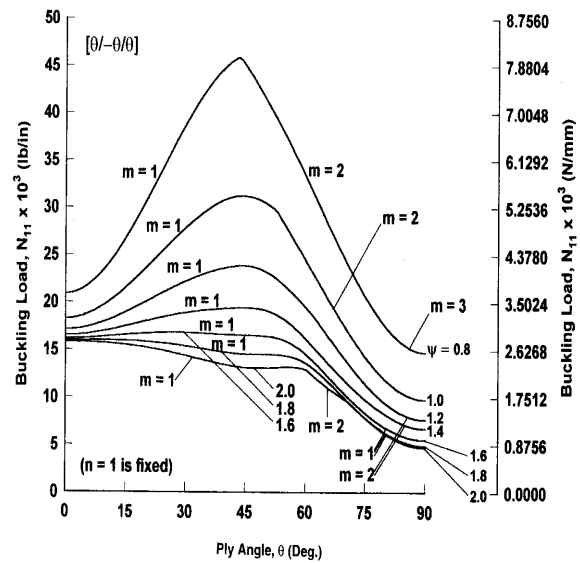


Fig. 5 The influence of the fiber orientation in the face-sheets on the uniaxial compressive buckling strength of a circular cylindrical sandwich panel with three layered facings. All four edges are freely movable and simply supported. ($L_1 = 24$ in., $h_f = 0.06$ in., $h_c = 0.5$ in., $R_2 = 100$ in., Materials F1:C1)

8 Postbuckling Response of Sandwich Panels

The effect of the ply-angle of the material of the face-sheets upon the edge load-center deflection interaction of a uniaxially compressed sandwich panel is depicted in Fig. 6. Herein the top and bottom face-sheets are made up of a single layer, each of the material F1.

The results reveal that the buckling bifurcation loads identified by the filled circles on the ordinate increase to ply-angle of 45 deg., after which, as the ply-angles increases, the buckling load decreases.

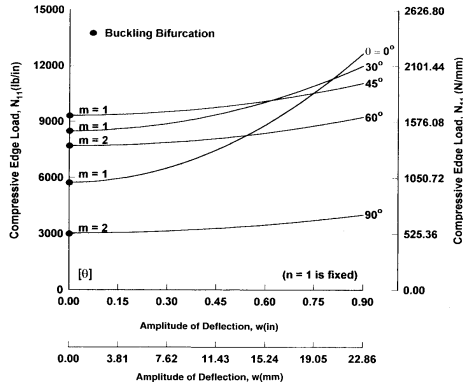


Fig. 6 Load-deflection amplitude interaction for a uniaxially compressed flat sandwich panel, whose face-sheets are made up each from one layer. ($L_1 = L_2 = 24$ in., $h_f = 0.02$ in., $h_c = 0.5$ in., Materials F1:C1)

A similar trend can be seen in the deep post-buckling range. In Fig. 7 it is displayed the thermoelastic response of a doubly-curved sandwich panel each face-sheet being constructed of three layers in the sequence $[\theta/0^\circ/\theta]$. It is supposed that the structure is immersed in an increased antisymmetric through thickness temperature field, and that a fixed uniaxial compressive load is also present. Due to the compressive load, when $T_b = 0$, the panel exhibits an initial upward (negative) deflection. However with the increase of T_b , the upward deflection tends to decrease, and at a certain temperature, a limit temperature is experienced. Its further increase is followed by a snapping jump. The results displayed in this figure reveal that for selected values of the ply-angle the intensity of the snap-through jump can be attenuated and even its occurrence removed.

It can be stressed here that in contrast to the standard homogeneous or laminated curved panels, in the case of their sandwich counterparts, the snapping phenomenon occurs in extreme loading only conditions.

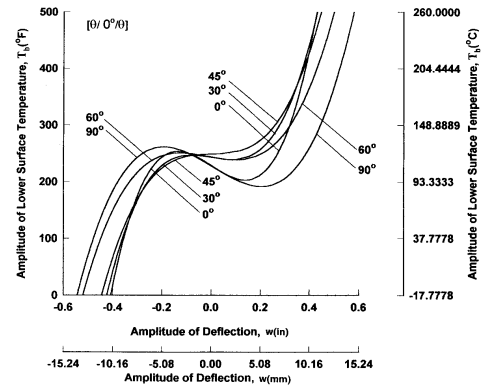


Fig. 7 The nonlinear response of a doubly curved sandwich panel with three layered face-sheets subjected to a fixed compressive edge preload and a temperature rise T_b . All four edges are movable and simply supported. ($L_1 = L_2 = 24$ in., $h_f = 0.45$ in., $h_c = 0.25$ in., Materials F1:C2)

This dramatic departure from the usual behavior of homogeneous/laminated curved panels whose load carrying capacity is imperfection sensitive, is due to the large overall bending stiffness provided by the core layer.

For more extended results that can offer a wider picture of the implications of a number of important effects on the buckling and non-linear response of flat and curved sandwich panels, the reader is referred to Refs. 7 through 10.

9 Conclusions

A number of results addressing both the modeling and the behavior of curved and flat sandwich panels with anisotropic face-sheets subjected to uni/biaxial edge loads, and an antisymmetric temperature gradient through panel wall-thickness have been presented. The material of each constituent laminae of the face-sheets was considered to feature monoclinic properties induced by the rotation of the fibers in each constituent ply with respect to the axes of the structure. The obtained results indicate that the directionality property of facings can play a tremendous role toward enhancing the buckling strength and the load carrying capacity in the postbuckling range. The implications of elastic characteristics of materials of face-sheets and of the core

on the buckling and postbuckling strength have been highlighted and their important role of enhancing the buckling strength and the postbuckling response behavior has been emphasized.

Moreover, it was shown that in some complex loading conditions, when the snap-through buckling can emerge, a judicious use of the directional properties of the material of face-sheets can result in the attenuation of its intensity, and even of its elimination altogether.

10 Acknowledgment

The work reported herein was supported in part by NASA Langley Research Center under Grant NAG-1-1689.

References

- [1] Noor, A.K., Burton, W.S., Bert, C.W., "Computational models for sandwich panels and shells," *Applied Mechanics Reviews*, Vol. 4, No. 3, March, 155-199, 1996.
- [2] Librescu, L. and Hause, T., "Recent development in the modeling and behavior of advanced sandwich constructions: a survey," *Journal of Composite Structures*, **48**, 1-3, pp. 1-17. 1999.
- [3] Librescu, L., "On a bending theory of elastic anisotropic sandwich-type panels," *Doklady Akademi Nauk SSR*, 182, 1, pp. 60-63, 1987 (Moscow, (Translated into English, Soviet Physics-Doklady, Vol. 13, (1969), 957-959).
- [4] Librescu, L., "Bending theory of elastic anisotropic sandwich plates," *Revue Roumaine des Sciences Techniques-Mecanique Appliquee*, 14, 1, pp. 137-149, 1969.
- [5] Librescu, L., "On a geometrically non-linear theory of elastic anisotropic sandwich-type plates," *Revue Roumaine des Sciences Techniques-Mecanique Appliquee*, 15, 2, pp. 323-339, 1970.
- [6] Librescu L., *Elastostatics and Kinetics of Anisotropic and Heterogeneous Shell-Type Structures*, Chapters V-VII, 493-540, Noordhoff International Publishers, Leyden, The Netherlands, 1975.
- [7] Librescu, L., Hause, T., and Camarda, C. J., "Geometrically nonlinear theory of initially imperfect sandwich plates and shells incorporating non-classical effects," *AIAA Journal*, Vol. 35, No. 8, pp. 1393-1403, 1997.
- [8] Hause, T., Librescu, L. and Camarda, C. J., "Postbuckling of anisotropic flat and doubly-curved sandwich panels under complex loading conditions," *International Journal of Solids and Structures*, pp. 3007-3028, 1998.
- [9] Hause, T., Johnson, T. F. and Librescu, L., "Effect of face-sheet anisotropy of buckling and postbuckling of flat sandwich panels," *Journal of Spacecraft and Rockets*, Vol. 37, No. 3, pp. 331-341, 2000.
- [10] Hause, T., Librescu, L. and Johnson, T. F., "Nonlinear response of geometrically imperfect flat and curved sandwich panels subjected to thermomechanical loading," *International Journal of Non-Linear Mechanics*, Vol. 33, No. 6, November, pp. 1039-1059, 1998.
- [11] Librescu, L., "Refined geometrically non-linear theories of anisotropic laminated shells," *Quarterly of Applied Mathematics*, Vol. 45, No. 1, pp. 1-22, 1987.
- [12] Librescu, L., and Stein M., "Postbuckling behavior of shear deformable composite flat panels taking into account geometrical Imperfections," *AIAA Journal*, Vol. 30, May, pp. 1352-1360, 1992.
- [13] Librescu, L., Lin, W., Nemeth, M.P., and Starnes J.H., Jr. "Classical versus non-classical postbuckling behavior of laminated composite panels under complex loading conditions," in *Non-Classical Problems of the Theory and Behavior of Structures Exposed to Complex Environmental Conditions*, AMD-Vol. 164, ASME, Ed. L. Librescu, pp. 169-182, 1993.